International Journal of Offshore and Coastal Engineering
Vol.10 | No. 1 | pp. 45 – 55 | May 2026
e-ISSN: 2580-0914

Submitted: November 22, 2025 | Revised: February 17, 2016 | Accepted: April 8, 2026

Line Clashing Probability Analysis of Catenary Anchored Leg Mooring with Quadraple Marine Hose Configuration

Gumilang Alhafiz[a,*], Murdjito[a] and Eko Budi Djatmiko[a], Fajar Rachmadiarto[b]

[a)] Department of Ocean Engineering, Sepuluh Nopember Institute of Technology, Surabaya 60111

[b)]PT. ZEE Indonesia

*Corresponding author: gumilangah@gmail.com

ABSTRACT

Global efforts to reduce carbon emissions have encouraged the adoption of lighter and more flexible offshore structures in support of Sustainable Development Goal (SDG) 13 and the International Maritime Organization (IMO) climate initiatives. This study investigates the technical performance of a Catenary Anchored Leg Mooring (CALM) terminal system connected to a Floating Storage and Offloading (FSO) facility using four subsea hose configurations of the Chinese lantern and lazy S types. Due to their flexibility, subsea hoses are susceptible to clashing under extreme environmental conditions, potentially causing damage and reducing operational reliability. Dynamic simulations were conducted to evaluate tensile forces, minimum bending radius, bending moments, shear forces, torsion moments, and the probability of hose clashing. Prior to the analysis, buoy stability was assessed following modifications to the hose configuration. The results indicate that the additional hose arrangement increased the buoy draft by 14.9% to 2.73 m. Under Accidental Limit State (ALS) conditions caused by anchor chain failure, structural loads on the hoses increased significantly, while the minimum bending radius decreased by 6%. Furthermore, the probability of hose clashing was substantially higher in ALS conditions than in Ultimate Limit State (ULS) conditions, demonstrating that anchor chain failure significantly increases the risk of subsea hose interaction and potential damage.

Keywords: *Stability, Subsea Hose, Line Clashing, Probability*

1. INTRODUCTION

Hydrocarbons have driven economic growth for 150 years, but emissions from hydrocarbons can disrupt the Earth's climate stability. The impact of fossil fuels on the Earth's atmospheric conditions has been widely recognized [14]. The Indonesian government has committed to reducing greenhouse gas emissions (GHG) from fossil fuel consumption as part of its efforts to address climate change [2].

A solution to reduce carbon emissions in offshore oil and gas operations is by using CO2 gas reinjection solutions into seabed geological formations [14]. In this context, PT. XYZ plans to implement a similar scheme in its mooring terminal system. Therefore, this study investigates the mooring terminal using a Single Point Mooring (SPM) system with a Catenary Anchored Leg Mooring (CALM) buoy and subsea hose configurations of the Chinese lantern and lazy S types, which are anchored to a Floating, Storage, and Offloading (FSO) facility. Due to their flexible nature, clashing between subsea hoses can occur under extreme environmental conditions. The clashing phenomenon can cause, among other things, damage to the outer layers of subsea hoses and failures due to repeated clashing impacts [10]. Based on this phenomenon, it is necessary to analyze the probability of clashing due to the use of four subsea hoses. This study simulates dynamic simulations and then analyzes the tensile forces, minimum bending radius, bending moment, shear forces, and torsion moments produced, as well as the potential for clashing between the subsea hoses and between subsea hoses and mooring lines. On the other hand, before conducting dynamic simulations, it is necessary to check the stability of the buoy structure due to modifications from its existing configuration..

2. LITERATURE REVIEW

The increasing demand for oil as an energy source has driven the development of floating offshore structures for exploration and exploitation activities at various water depths [13]. This has led to a growing trend for lighter and more flexible floating structures for operational activities like fluid transportation, such as flexible risers [2]. There have been several innovations in floating structure designs aimed at efficient fluid transportation, one of which is the Catenary Anchored Leg Mooring (CALM) system [17]. Generally, CALM buoys are floating offshore structures that exhibit motion responses in six degrees of freedom (6 DOF) [11] and are typically tethered using mooring lines [16]. These buoys are connected to floating hoses, subsea hoses, and reeling hoses that are highly efficient in fluid transport. However, these hoses are vulnerable to failures due to clashing and limitations in strength [18]. Several studies have been conducted to investigate the configuration of subsea hoses concerning strength criteria parameters. In other side, The strength of subsea hoses and mooring systems in Single Point Mooring (SPM) setups due to variations in the number of subsea hoses. The results indicated that the maximum mooring line tension is greatly influenced by the movement of the Floating, Storage, and Offloading (FSO) unit and environmental loading direction, resulting in an increase of up to 86.13% under ultimate conditions [15]. Meanwhile, the maximum subsea hose tension decreases when additional hoses are added to the system. Despite these studies, research on the impact of adding subsea hose configurations on the probability of clashing has not been extensively explored. Recent studies have only started addressing the prediction of clashing probabilities in systems with two riser configurations. Therefore, this research aims to analyze the probability of clashing in subsea hoses resulting from the addition of subsea hose configurations.

3. METHODOLOGY

3.1 FSO Data

In operating the ABC Terminal, PT. XYZ uses FSO X for storage and offloading activities. Alongside this, FSO X is utilized as one of the research objects in this study to address the formulated research questions. The main dimensions of FSO X are shown in Table 1.

Table 1 FSO X Principal Dimension

Parameter	Data		Unit
	Light Ship	*Full Load*	
Length	142.6		m
Breadth	48.2		m
Depth	26.5		m
Draft	2.5	24	m
Displacement	15529	153202	ton

3.2 Buoy Data

During its operational period, FSO X will be moored using an SPM Buoy to ensure it remains in the desired position. The main dimensions of the SPM buoy structure are shown in Table 2.

Table 2. SPM Buoy Principal Dimension

Parameter	Data	Unit
Outer Diameter	12	m
Centre Well Diameter	3.57	m
Buoy Body Height	5.3	m
Skirt Outer Diameter	16.26	m
Skirt Height	1	m
Buoy Installed Draft	2.38	m
Centre of Gravity (KG)	3.42	m
Displacement	253.83	tonne

3.3 Mooring Data

To provide a restoring force to the FSO when it experiences motion responses due to environmental loads, the FSO Arco Ardjuna is moored using hawser lines connected to a CALM buoy with a catenary anchor chain configuration. The properties of the anchor chain and hawser lines are detailed in Table 3 and

Table 4.

Table 3. Mooring Chain Properties

Parameter	Data	Unit
Configuration	6 × 1	-
Diameter	0.102	m
Material	Studlink – Grade 3 (R3)	-
Minimum Breaking Load (MBL)	8315	kN
Pre-Tension	26217	kN
Length	350	m
Weight in Air	210.16	kg/m

Table 4. Mooring Hawser Properties

Parameter	Data	Unit
Configuration	2 × 1	-
Diameter	0.158	m
Material	Nylon OCIMF 2000	-
Minimum Breaking Load (*Dry*) (MBL)	4904	kN
Length	70	m
Weight in Air	16.17	kg/m

3.4 Subsea Hose Data

The specifications of the subsea hose used for one string of subsea hose in this study are shown in Table 5 below. The hose section configuration in this study is based on the Flexomarine catalog.

Table 5. Subsea Hose Arrangements

Description	Data	Unit
	Chinese Lantern	
Hose section	4	ea
Total length	42.8	m
Arrangement	1. *Reinforced End* (SPM) 2. *Submarine Line* 3. *Submarine Line* 4. *Reinforced End* (PLEM)	kN
No. of *floater*	2 (I.D. 697)	ea (mm)
	4 (I.D. 581)	ea (mm)
	Lazy S	
Hose section	6	ea
Total length	64.2	m
Arrangement	1. *Reinforced End* (SPM) 2. *Submarine Line* 3. *Submarine Line* 4. *Reinforced End* (PLEM)	kN
No. of *floater*	4 (I.D. 697)	ea (mm)
	3 (I.D. 581)	ea (mm)

Table 6. Subsea Hose Section Properties

Parameter	Data			Unit
Name	First-off Buoy Hose	Mainline Hose	First-off PLEM	-
Section	1st Section	2nd Section	3rd Section	-
Hose Type	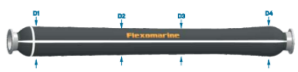	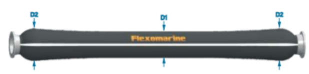	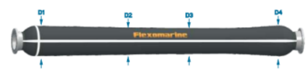	
Body Array	V1 (Hose Fitting) V1 (Reinforced End) V1 (Hose Body) V1 (Hose End) V1 (Hose Fitting)	V2 (Hose Fitting) V2 (Hose End) V2 (Hose Body) V2 (Hose End) V2 (Hose Fitting)	V3 (Hose Fitting) V3 (Hose End) V3 (Hose Body) V3 (Reinforced End) V3 (Hose Fitting)	- - - - -
Type	Single Carcass	Single Carcass	Single Carcass	-
Nominal Bore	16 406.4	16 406.4	16 406.4	in mm
Standard Length	10.7	10.7	10.7	m
Minimum Bending Radius	64	64	64	in
Density	1.1	1.1	1.1	ton/m
Weight	0.13	0.13	0.13	ton/m
Axial Stiffness	11550	11550	11550	kN
Bending Stiffness	16	16	16	kN.m^2
Torsional Stiffness	480	480	480	kN.m^2

3.5 Environmental Data

Before conducting the analysis, it is essential to understand the real conditions in the field related to the system that will be analyzed. Given that FSO X, operating at Terminal ABC, is stationary or remains at the operational location for an extended period (fixed), it is assumed that under extreme conditions, FSO X will remain moored to the SPM buoy. Wave, wind, and current data at the location where FSO X operates are obtained using actual data from the relevant terminal. Wave period data for input in the numerical simulation is estimated according to [12].

With environmental load conditions assumed to be omnidirectional, several loading scenarios have been determined for various wave, wind, and current directions. Since all anchor chains have identical properties with a symmetrical mooring configuration and the weathervaning capability of the SPM system, there is no need to analyze environmental loads from directions 0° to 360°. Therefore, only the analysis of inline and between line environmental loading conditions relative to the anchor chains is required. The inline loading direction will align with the inflow direction towards the Chinese lantern configuration, while the between line direction will align with the crossflow direction towards the lazy S configuration. The variations in environmental load directions are comprehensively presented in Table 7. Furthermore, all variations will be analyzed under both full load and light ship conditions of the

FSO, for both operational and extreme conditions, at a sea depth of 45 meters referenced to MSL. The total number of loading scenarios to be analyzed is 24.

Table 7. Environmental Loading Scenario

No.	Description	Incident[Chain]	Incident [CL]	Incident [LS]	Wave (°)	Wind (°)	Current (°)
1.	*Collinear*	*Inline*	*Cross flow*	*Inflow*	0	0	0
2.	*Collinear*	*Between line*	*Inflow*	*Cross flow*	0	30	30
3.	*Non-collinear 1*	*Inline*	*Cross flow*	*Inflow*	0	45	30
4.	*Non-collinear 1*	*Between line*	*Inflow*	*Cross flow*	90	90	90
5.	*Non-collinear 2*	*Inline*	*Cross flow*	*Inflow*	90	120	120
6.	*Non-collinear 2*	*Between line*	*Inflow*	*Cross flow*	90	135	120

4. RESULTS AND DISCUSSION

4.1 FSO & Buoy Modelling

The re-modeling process begins with modeling the hull shape of the FSO and buoy using input in the form of the main dimensions of FSO X and the buoy. Then, the model will be validated against hydrostatic parameters. This modeling and hydrostatic analysis process is carried out iteratively until the hydrostatic parameters meet the validation criteria. The results of the re-modeling of FSO X and the buoy are shown in Figure 1.

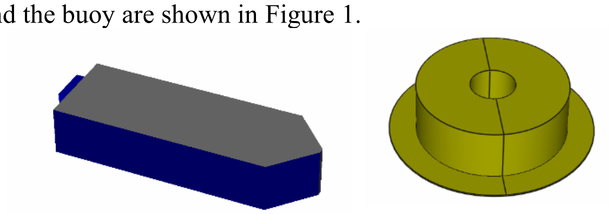

Figure 1. Modeling FSO X and SPM Buoy

The validation criteria used refer to the ABS – Rules for Building and Classing Marine Vessels (2023). According to the ABS – Rules for Building and Classing Marine Vessels (2023), several hydrostatic parameters must be validated against the stability booklet, namely displacement, LCB, LCF, KB, and KMT. On the other hand, this study has limitations regarding buoy data, so the validation criteria will only be applied to the displacement parameter. The validation of the FSO X and SPM Buoy models is shown in Table 8, Table 9, and Table 10.

Table 8. Model Validation of FSO X (Full Load)

Parameter	Data	Model	Unit	Error	Remarks
Displacement	153202	153352	ton	0.1%	PASS
LCB from MS (+ve aft)	2.782	3.022	m	0.24	PASS
LCF from MS (+ve aft)	2.795	3.023	m	0.23	PASS
KB	12,03	12	m	0.03	PASS
KMT	19.73	19.761	m	0.16%	PASS

Table 9. Model Validation of FSO X (Light Ship)

Parameter	Data	Model	Unit	Error	Remarks
Displacement	15529	15479	ton	0.32%	PASS
LCB *from MS (+ve aft)*	2.68	2.283	m	0.397	PASS
LCF from MS (+ve aft)	2.76	2.283	m	0.477	PASS
KB	1.271	1.25	m	0.02	PASS
KMT	76.757	76.08	m	0.88%	PASS

Table 10. Model Validation of SPM Buoy

Parameter	Data	Model	Unit	Error	Remarks
Displacement	253.83	258.8	ton	1.95%	PASS

Based on the table above, the parameters tested for validity meet the criteria of the ABS – Rules for Building and Classing Marine Vessels (2023). The displacement and keel to transverse metacenter parameters show a maximum difference of 0.32% and 0.88%, respectively, compared to the stability booklet data. For the validation of weight points, such as the longitudinal center of buoyancy (LCB), floatation (LCF), and keel to center of buoyancy (KB), the validation criteria involve comparing the differences between the hydrostatic parameter outputs and the stability booklet data. The maximum differences for LCB, LCF, and KB parameters are 0.397 m, 0.477 m, and 0.03 m, respectively, indicating that the FSO model can be used for further analysis. For the SPM buoy, the displacement parameter in the SPM buoy modeling also meets the criteria of the ABS – Rules for Building and Classing Marine Vessels (2023), with a maximum displacement difference of 1.95% compared to the buoy's primary data.

4.2 Hydrodynamics Analysis

Simulations of the FSO's motion response are conducted to understand its characteristics in free-floating conditions with regular waves. Before performing hydrodynamic analysis, it's necessary to carry out 3D diffraction modeling of the FSO. The 3D diffraction model, depicted in Figure 2, will then undergo hydrodynamic analysis to provide inputs for dynamic analysis in software like OrcaFlex.

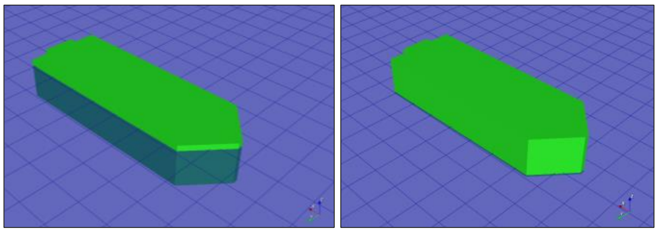

Figure 2 Model 3D Diffraction of FSO X

The simulation is conducted at a ship speed of 0 m/s because FSO X operates as a stationary structure. The goal is to obtain outputs such as hydrodynamic parameters of the structure, including motion RAO (Response Amplitude Operator), load RAO, wave drift QTF (Quadratic Transfer Function), added mass, and damping matrix. The results from this analysis will serve as inputs for dynamic simulations in random waves, incorporating the mooring system configuration, using software like OrcaFlex.

4.3 Mooring System & Subsea Hose Modelling

The buoy structure is modeled into five main components: buoy body, turntable part, skirt, chain stopper, and center well. The buoy body and skirt are defined as a 6-degree-of-freedom (6 DOF) buoy, allowing free movement in six degrees of freedom and accommodating hydrodynamic properties. The modeling of the anchor chain and hawser is adjusted based on the material properties used in real field conditions, such as diameter, axial stiffness, and weight. An illustration of the mooring system modeling including the buoy and FSO overall can be seen in Figure 3 and Figure 4.

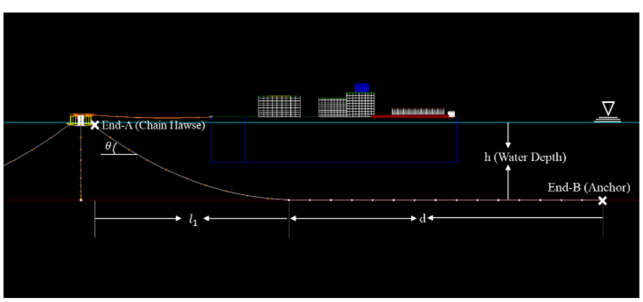

Figure 3 Mooring System Modeling (*Side View*)

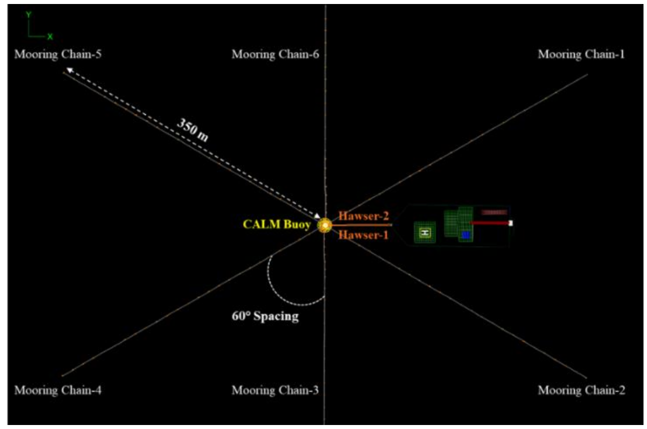

Figure 4 Mooring System Modeling (*Top View*)

In the dynamic simulations, the anchor chains will be subjected to environmental loads inline and between line, while the subsea hoses will experience environmental loads in inflow and crossflow directions, as illustrated in Figure 5 and Figure 6.

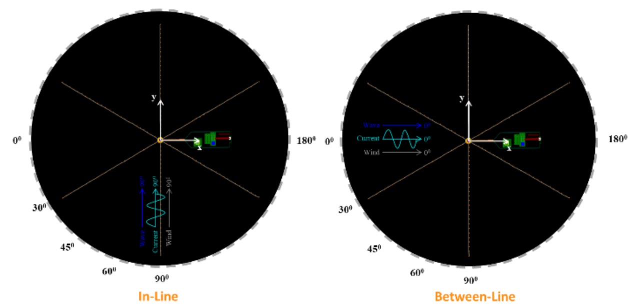

Figure 5 Loading Scenario Relative to Mooring Chain

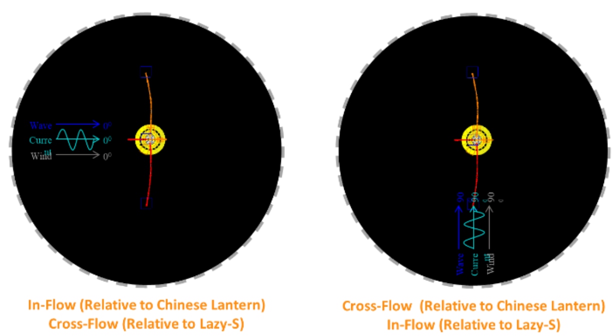

Figure 6 Loading Scenario Relative to Subsea Hose

Furthermore, prior to conducting dynamic analysis, this study did not investigate the impact of varying the number of floaters but rather focused on studying variations in floater or buoyancy module spacing. Figure 7 depicts a schematic design of the subsea hose modeling for Lazy S and Chinese Lantern configurations. Reinforced hoses and submarine line hoses are represented by black lines to match the physical color of the subsea hoses. Orange-colored circles indicate buoyancy modules (body floaters), and gray segments represent flanges.

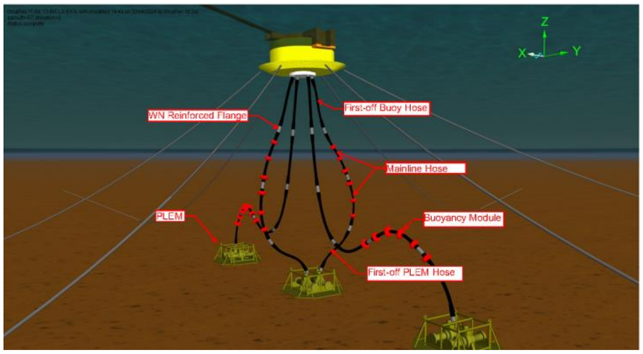

Figure 7 Subsea Hose Modeling

4.4 Buoy Stability Analysis

Before conducting buoy stability analysis due to the addition of subsea hose configurations, a static analysis is necessary to determine changes in buoy draft. Subsequently, the draft output from the static simulation in OrcaFlex software will be used as input for buoy stability analysis in MAXSRUF Stability software. The draft of the modified SPM buoy condition is illustrated in Figure 8 below.

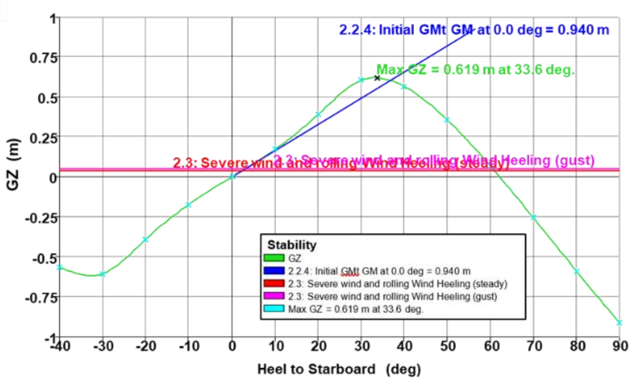

Figure 8 SPM Buoy Modification Stability Curve

Based on the stability analysis conducted, the stability of the modified SPM buoy condition meets the criteria of IMO MSC.267(85) Adoption of The International Code on Intact Stability 2008. A summary of the stability analysis results for the modified buoy is shown in Table 11. Following the buoy stability analysis under modified conditions, it can be concluded that with the addition of the riser configuration, the buoy experiences a draft increase of 14.9% and a decrease in GZ value by 48% compared to the existing buoy condition. Factors influencing the difference in GZ value include increased displacement and changes in the buoy's Center of Gravity (CoG) position.

Table 11. Summary of Buoy Stability Validation

IMO Criteria	Result	Criteria	Unit	Remarks
Statical Stability				
Area under GZ curve at 0 up to 30-degrees of heel angle	0.15	0.055	meter-radian	PASS
Area under GZ curve at 0 up to 40-degrees of heel angle	0.25	0.09	meter-radian	PASS
Area under GZ curve between 30 to 40 degrees of heel angle	0.10	0.03	meter-radian	PASS
Righting lever GZ at 30-degree of heel angle	0.61	0.2	meter	PASS
Heel Angle at maximum GZ	33.60	30	deg	PASS
Initial GM value	0.94	0.5	meter	PASS
Dynamical Stability				
Angle of Steady Heel	2.20	12	deg	PASS
Angle of Steady Heel / Deck Edge Immersion Angle	10.56	80	%	PASS
Area 1 / Area 2	796.35	100	%	PASS

4.5 Mooring Strength Analysis

Summary of simulations under intact and damaged conditions with outputs of maximum tension on anchor chains and hawsers are shown in Table 12 and Table 13. Based on the maximum tension results, the anchor chains comply with acceptance criteria from API RP 2 SK, and the hawsers comply with ABS – Position Mooring (2022) standards.

Table 12. Summary of Mooring Chain Maximum Tension

Scenario	Max. Chain Tension (kN)	Criteria (kN)	SF	Remarks
ULS	**3418.71** (Chain-3)	<4385.06 (60% MBL)	2.13	Comply API RP 2SK
ALS	**3889.16** (Chain-5)	<5846.75 (80% MBL)	1.87	Comply API RP 2SK

Table 13. Summary of Hawser Maximum Tension

Scenario	Max. Chain Tension (kN)	Criteria (kN)	SF	Remarks
ULS	**598.06** (Hawser-2)	>2.5 (Allowable S.F)	6.85	Comply ABS
ALS	**803.82** (Hawser-2)	>2.5 (Allowable S.F)	5.09	Comply ABS

4.6 Subsea Hose Analysis

Next, a comparison of dynamic simulation results under intact and damaged conditions for parameters of forces and moments on the subsea hoses is presented in Figure 9, Figure 10, Figure 11, Figure 12, and Figure 13.

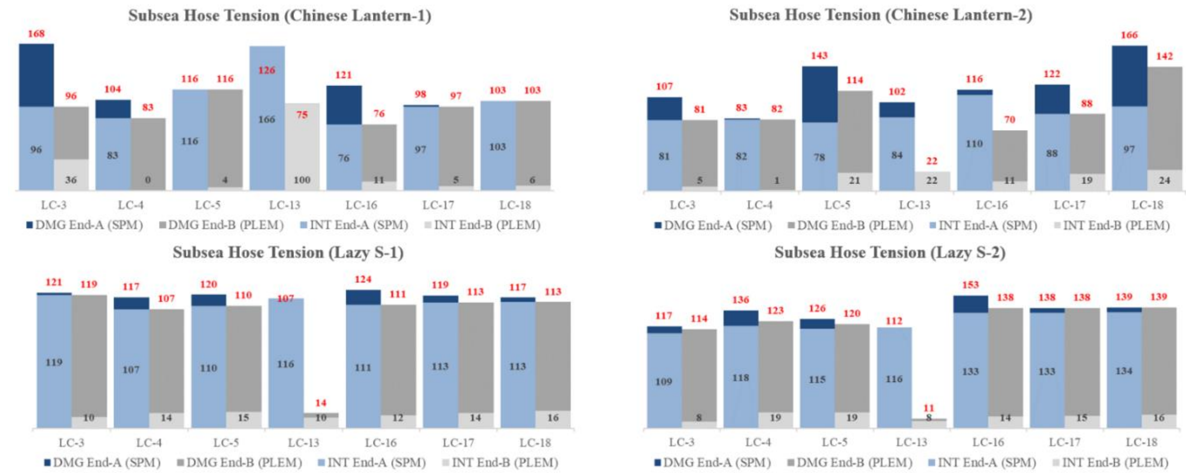

Figure 9 Comparison of Tension Force at Subsea Hose During Intact and Damage Condition

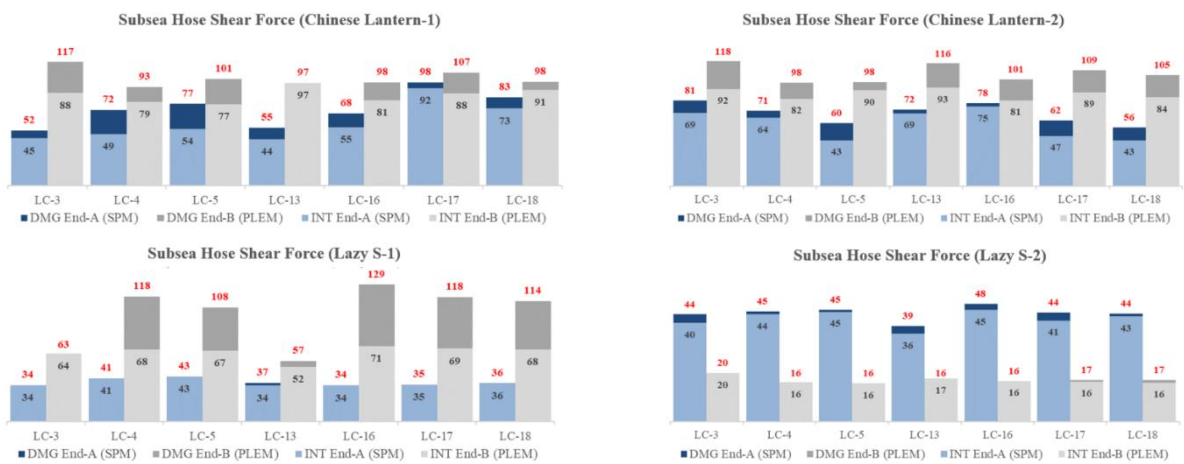

Figure 10 Comparison of Shear Force at Subsea Hose During Intact and Damage Condition

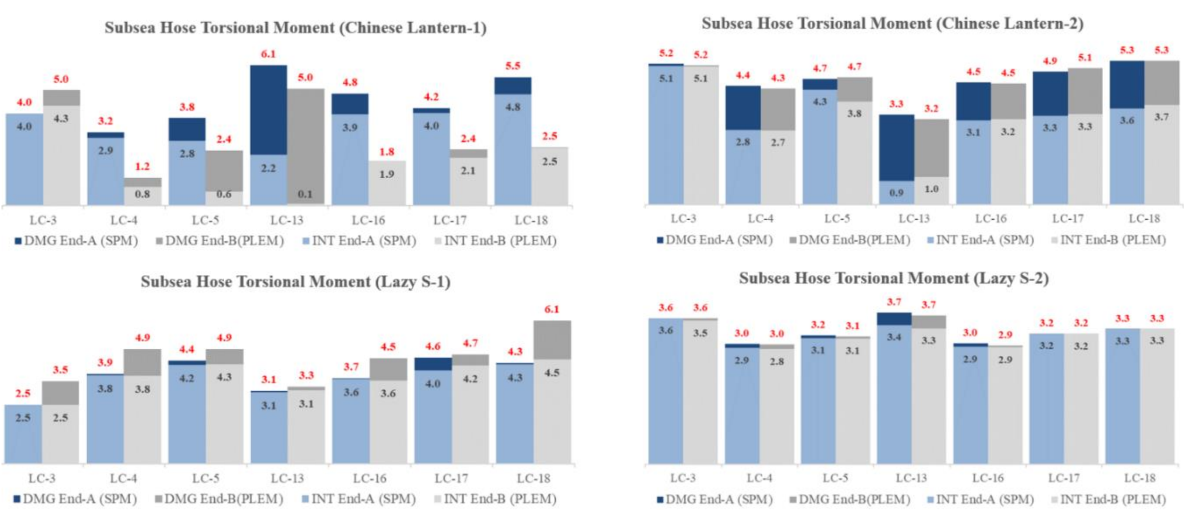

Figure 11 Comparison of Torsional Moment at Subsea Hose During Intact and Damage Condition

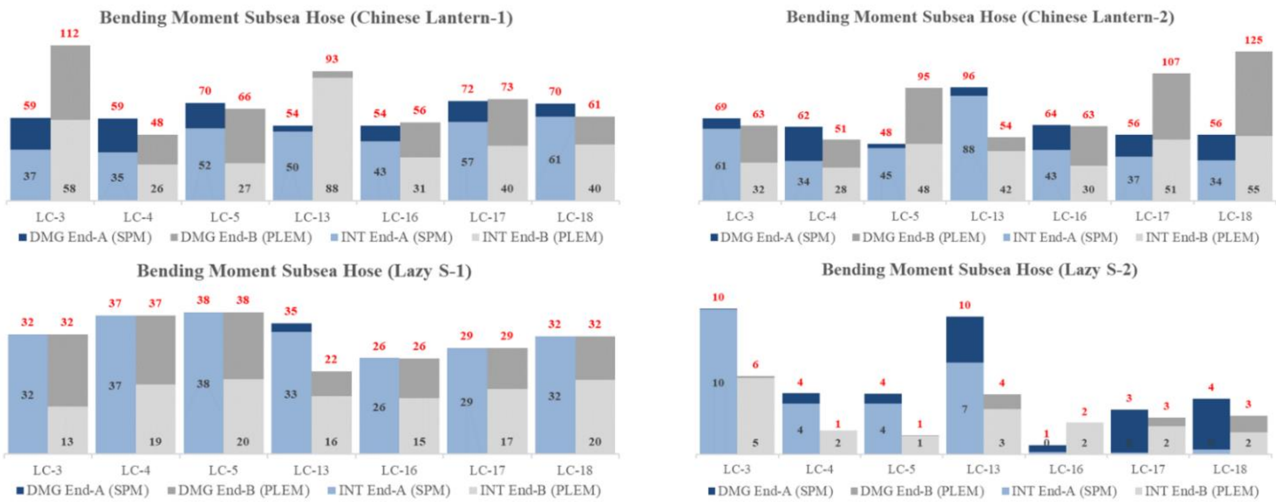

Figure 12 Comparison of Bending Moment at Subsea Hose During Intact and Damage Condition

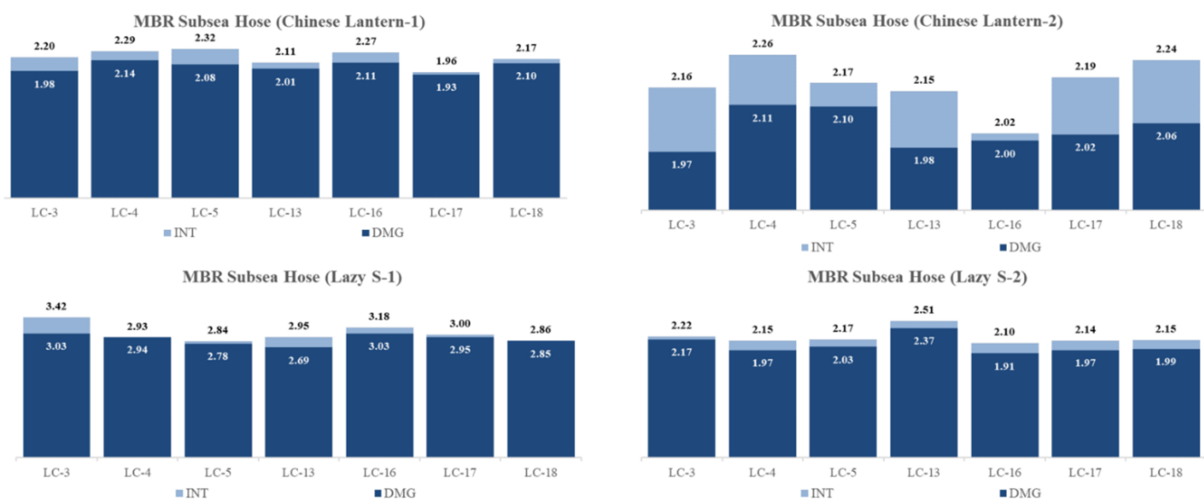

Figure 13 Comparison of Minimum Bending Radius at Subsea Hose During Intact and Damage Condition

Based on the comparison of forces and moments occurring on the subsea hoses, overall, the ALS condition results in an increase in bending moment, tension force, torsional moment, and shear force on the subsea hose at end-A (SPM) by 8%, 1%, 4%, and 4%, respectively. Meanwhile, the increase in bending moment, tension force, torsional moment, and shear force on the subsea hose at end-B (PLEM) is 30%, 29%, 4%, and 25%, respectively. On the other hand, the ALS condition leads to a decrease in the bending radius of the subsea hose by 6%.

4.6 Line Clashing Probability Analysis

In OrcaFlex, the subsea hose is modeled as a line element represented by a series of segments and nodes, corresponding to its properties and geometry. To analyze the probability of line clashing, the clearance between nodes on the subsea hose needs to be known. During dynamic analysis, the smallest clearance is defined as the distance between nodes on the subsea hose for each time series, denoted as $L_d(t)$. In this context, clashing occurs when the clearance is negative, or in other words, $L_d(t) < 0\,m$. However, considering safety factors, the minimum allowable clearance in this thesis is set to 2 times the outer diameter (OD) of the subsea hose, as stipulated by DNV-RP-F203 "Riser Interference". Therefore, for the purposes of this research, it is assumed that clashing of the subsea hose may occur when $L_d(t) < 1.25\,m$.

If the subsea hose experiences clashing with relatively high frequency, it can affect the strength and integrity of the subsea hose. Therefore, this thesis calculates the probability of clashing occurring in anchor chain conditions under intact and damaged states. For the intact condition, loading scenario LC-13 for subsea hose CL-2 was selected because in this scenario, CL-1 experienced 329 occurrences where node 40 had clearance values below the criteria of less than 1.25 meters, occurring randomly during a 3-hour simulation period. Meanwhile, for the damaged condition, loading scenario LC-18 for subsea hose CL-1 was chosen because in this scenario, CL-1 experienced 691 occurrences where node 58 had clearance values below the criteria of less than 1.25 meters, occurring randomly during a 3-hour simulation period. A detailed summary of occurrences where nodes on the subsea hose had clearance values below the criteria is presented in Table 14.

Table 14. Summary Clashing Sample on Subsea Hose

Scenario	Clashing Sample			
	CL-1	Cl-2	LS-1	LS-2
Intact				
3-INT-FL-EX-IL	Pass	304	293	Pass
4-INT-FL-EX-BL	Pass	Pass	Pass	Pass
5-INT-FL-EX-BL	Pass	Pass	Pass	Pass
13-INT-LS-EX-IL	8	329	Pass	293
16-INT-LS-EX-BL	Pass	Pass	Pass	Pass
17-INT-LS-EX-BL	10	Pass	11	Pass
18-INT-LS-EX-BL	21	Pass	25	Pass
Damage				
3-DMG-FL-EX-IL	Pass	150	432	Pass
4-DMG-FL-EX-BL	Pass	11	11	Pass
5-DMG-FL-EX-BL	34	Pass	34	Pass
13-DMG-LS-EX-IL	33	10	10	Pass
16-DMG-LS-EX-BL	36	46	43	Pass
17-DMG-LS-EX-BL	10	7	98	Pass
18-DMG-LS-EX-BL	691	1	664	Pass

After obtaining sample event information for potential clashing occurrences, a distribution test is necessary to determine the appropriate distribution based on the available sample data. To select the most suitable distribution, evaluation includes Anderson-Darling values and correlation coefficients obtained through statistical analysis, as presented in Table 15 and Table 16.

Table 15. Goodness-of-Fit at Intact Condition

Distribution	Anderson-Darling	Corrleation Coefficient
Weibull	26.347	0.998
3-Parameter Weibull	36.395	0.994
Normal	108.752	0.992
Lognormal	486.961	0.955
3-Parameter Lognormal	109.883	0.992
Logistic	127.532	0.992
Loglogistic	429.358	0.962
3-Parameter Loglogistic	128.606	0.992

Table 16. Goodness-of-Fit at Damage Condition

Distribution	Anderson-Darling	Correlation Coeficient
3-Parameter Lognormal	39.801	0.998
Logistic	190.240	0.990
Loglogistic	583.895	0.959
3-Parameter Loglogistic	190.644	0.990
Weibull	17.424	0.997
3-Parameter Weibull	10.720	1.000
Normal	39.074	0.998
Lognormal	597.024	0.955

The most suitable distribution for the sample data used in the analysis of clashing probabilities under intact conditions is the Weibull distribution because it has a lower Anderson-Darling value. Meanwhile, for the damaged condition, the Weibull distribution is also chosen as the most appropriate distribution due to its lower Anderson-Darling value and high correlation coefficient, demonstrating better fit with the available data. Further analysis aims to obtain the shape parameter, scale parameter, and threshold parameter for the probability analysis. Figure 14 and Figure 15depict the probability graphs of clashing occurrences for intact and damaged conditions using the Weibull distribution.

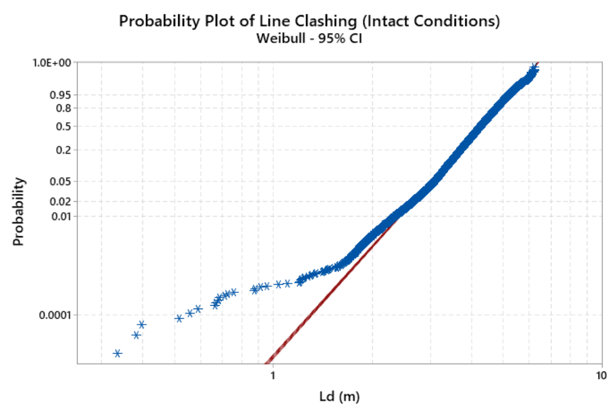

Figure 14 Clashing Distribution 3-Para Weibull (ULS)

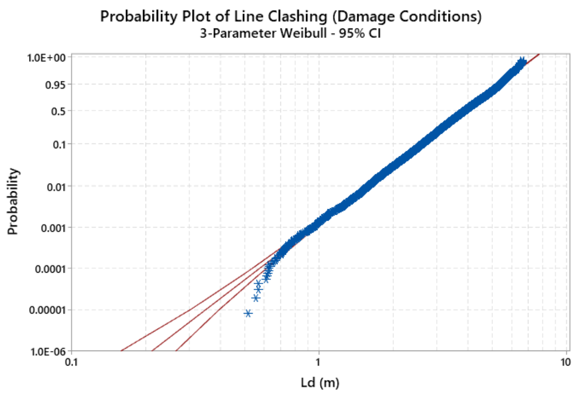

Figure 15 Clashing Distribution 3-Para Weibull (ALS)

After plotting the most suitable distribution for the data, the parameters of the Weibull distribution were determined to assess the probability of clashing occurrences using the probability density function graphs presented in Figure 16 and Figure 17.

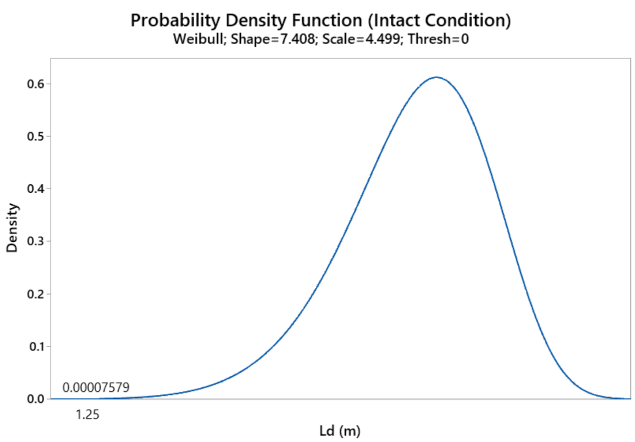

Figure 16 Line Clashing Probability Density Function (ULS)

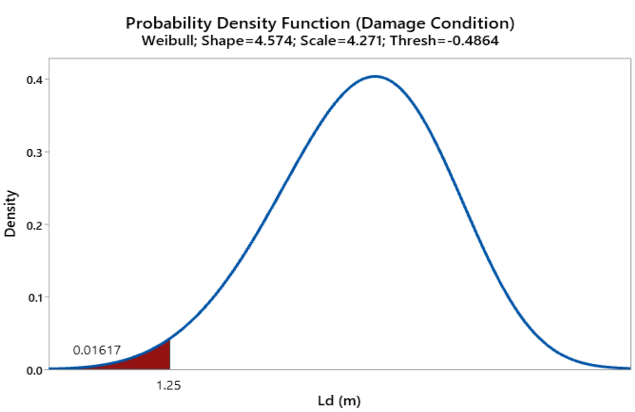

Figure 17 Line Clashing Probability Density Function (ALS)

Figure 16 depicts a distribution that is more centralized with a high and relatively narrow peak, indicating that in the intact condition, the clearance between subsea hoses exhibits relatively small variations around the center value. The center value refers to the value around which the data tends to cluster. In the probability density function (PDF) graph, the center value is the value on the horizontal axis (Ld) where the probability density reaches its peak. This represents the clearance value between subsea hoses that occurs most frequently within the data range or during the 3-hour simulation period. In other words, the clearance values in the intact condition show low variability, resulting in a relatively small probability of clashing, specifically 7.5×10^{-5}. On the other hand, Figure 17 shows a distribution that is wider with a lower peak, indicating that in the damaged condition, the clearance between subsea hoses is more variable relative to the center value compared to the intact condition. This implies that although there are more data samples with relatively large variations around the center value, or in other words, the clearance values in the damaged condition exhibit higher variability, the probability of clashing is relatively high, specifically 1.6×10^{-2}.

5. CONCLUSIONS

Based on the analysis conducted in this study, the following conclusions are drawn:

1. After conducting stability analysis for the intact condition of the existing buoy with a draft of 2.38m, a maximum GZ value of 1.21m was obtained at an angle of 34.5°. On the other hand, static analysis in Orcaflex yielded a draft of 2.735m for the modified buoy with a maximum GZ value of 0.619m at an angle of 33.6°. There was an increase in buoy draft by 14.9% and a decrease in GZ value by 48% compared to the existing buoy condition. Factors influencing the difference in GZ value include buoy displacement and CoG position due to the addition of riser configurations, directly affecting buoy stability.
2. Overall, the ALS condition resulted in an increase in bending moment, tensile force, torsional moment, and shear force on the subsea hose at connection end-A (SPM) by 8%, 1%, 4%, and 4%, respectively. Meanwhile, the increase in bending moment, tensile force, torsional moment, and shear force on the subsea hose at connection end-B (PLEM) was 30%, 29%, 4%, and 25%, respectively. On the other hand, the ALS condition led to a 6% decrease in bending radius of the subsea hose.
3. The probability of subsea hose line clashing in the mooring damage condition is higher compared to the intact condition, with probabilities of 7.5×10^{-5} and 1.6×10^{-2}, respectively. It is concluded that anchor chain failure increases the probability of line clashing by 21235%.

REFERENCES

[1] ABS. (2023). Rules for Building and Classing Marine Vessels. Houston, Texas USA: American Bureau of Shipping

[2] Amaechi, C. V., Gillett, N., Odijie, A. C., Hou, X., & Ye, J. (2019). Composite Risers for Deep Waters Using a Numerical Modelling Approach. Composite Structures, 210, 486–499.

[3] Amaechi, C. V., Wang, F., Hou, X., & Ye, J. (2019). Strength of Submarine Hoses in Chinese Lantern Configuration from Hydrodynamic Loads on CALM Buoy. Lancaster E-Prints.

[4] Amaechi, C. V., Chesterton, C., Butler, H. O., Wang, F., & Ye, J. (2021). An Overview on Bonded Marine Hoses for Sustainable Fluid Transfer and (Un)Loading Operations via Floating Offshore Structures (FOS). Journal of Marine Science and Engineering, 9(10).

[5] Amaechi, C. V., Wang, F., & Ye, J. (2022). Numerical Studies on CALM Buoy Motion Responses and the Effect of Buoy Geometry Cum Skirt Dimensions with its Hydrodynamic Waves-Current Interactions. Ocean Engineering, 244.

[6] Amaechi, C. V., Wang, F., & Ye, J. (2022b). Understanding the Fluid–Structure Interaction from Wave Diffraction Forces on CALM Buoys: Numerical and Analytical Solutions. Ships and Offshore Structures, 17(11), 2545–2573.

[7] Amaechi, C. V., Wang, F., & Ye, J. (2022). Investigation on Hydrodynamic Characteristics-Wave Current Interaction and Sensitvity Analysis of Submarine Hoses Attached to a CALM Buoy. Journal of Marine Science and Engineering, 10(1)

[8] API RP2SK. (2005). Recommended Practice for Design and Analysis of Station Keeping Systems for Floating Structures. Washington, D.C. : American Petroleum Institute.

[9] Bai, Y., & Bai, Q. (2005). Subsea Pipelines and Risers. Oxford: Elsevier.

[10] DNV GL-OS-E301. (2015). Position mooring. German: Det Norske Veritas Germaniscer Llyod

[11] Duggal, A., & Ryu, S. (2005). *The Dynamics of Deepwater Offloading Buoys*. Southampton: WIT Press

[12] Faltinsen, O. (1990). Sea Loads on Ships and Offshore Structures (1st ed.). Cambridge:Cambridge University Press.

[13] Islam, A. B. M. S., Jameel, M., Jumaat, M. Z., Shirazi, S. M., & Salman, F. A. (2012). Review of Offshore Energy in Malaysia and Floating Spar Platform for Sustainable Exploration. In *Renewable and Sustainable Energy Reviews* (Vol. 16, Issue 8, pp. 6268–6284). Elsevier.

[14] Ma, K.T., Luo, Y., Kwan, C.T.T., Wu, Y. Mooring System Engineering. (2019). Elsevier

[15] Rachman, R. D. (2023). *ANALISIS KEKUATAN SISTEM TAMBAT DAN SUBSEA HOSE PADA SINGLE POINT MOORING AKIBAT VARIASI JUMLAH SUBSEA HOSE*.

[16] Ricbourg, C., Berhault, C., Camhi, A., Lécuyer, B., & Marcer, R. (2006). *Numerical and Experimental Investigations on Deepwater CALM Buoys Hydrodynamics Loads*. Paper Presented at the Offshore Technology Conference, Houston, Texas, USA.

[17] Sun, L., Zhang, X., Kang, Y., & Chai, S. (2015). *Motion Response Analysis of FPSO'S CALM Buoy Offloading System.* Offshore and Arctic Engineering, 11. Newfoundland, Canada.

[18] Tonatto, M., Roese, P. B., Tita, V., Forte, M., & Amico, S. (2019). Offloading Marine Hoses:Computational and Experimental Analyses. In Marine Composites (pp. 391 - 415).